# 3-D Comparison of the shape and position of the condyle before and after Class II correction

**Sepideh Torkan**

A THESIS
SUBMITTED IN PARTIAL FULFILLMENT OF
THE REQUIREMENTS FOR THE DEGREE OF

MASTER OF SCIENCE IN DENTISTRY

**UNIVERSITY OF WASHINGTON**
**2018**

**COMMITTEE:**
Greg Huang
David Hatcher
Zi-Jun Liu

PROGRAM AUTHORIZED TO OFFER DEGREE:
DEPARTMENT OF ORTHODONTICS

University of Washington

## ABSTRACT

**3-D Comparison of the shape and position of the condyle before and after Class II correction**

SEPDIEH TORKAN

Chair of Supervisory Committee:
Greg J. Huang
Department of Orthodontics

**Introduction**: The aims of this study were to assess the changes in the shape and position of the condyle in the fossa as well as its position relative to the cranial base before and after Class II correction with the Herbst appliance (HA) or headgear (HG), and to also compare any changes to matched Class I cases.

**Methods**: Patients were divided into four groups, Class II treated with HA and their matched Class I cases, as well as Class II cases treated with HG and their matched Class I cases. CBCTs were obtained before and after treatment in all cases. A total of 122 condyles (left and right) from 61 patients were assessed. 242 landmarks were identified on the condyle and fossa, from which 3-D surface meshes were created. 7 relatively stable landmarks were recorded on the skull to assess the position of the condyle relative to cranial base. Length of the mandible was measured on laterals cephalograms rendered from CBCTs. Principal component, generalized Procrustes, and discriminant function analyses were used to assess shape and position changes.

**Results**: There were no significant changes in the position of the condyle relative to the cranial base before and after treatment. No significant differences were reported in the anteroposterior or vertical position of the condyle relative to the fossa (P=0.71 and P=079 respectively). There were significant changes in the shape of the condyles when Class II untreated cases were compared to controls. Untreated Class II cases had more internal rotation of the mediolateral long axis of the condyles when compared to Class I cases. There were no significant differences in changes in the length of the mandible between Class II and control cases.

**Conclusion**: The condyles of all untreated patients, whether they were Class I or Class II initially, did not change their position (within the fossa or relative to stable cranial base structures) when assessed at the end of orthodontic treatment.

**Table of contents**

# Introduction

Class II malocclusion is known to be the most common problem referred for orthodontic treatment (Nanda 2005), and many different appliances and techniques have been proposed to correct Class II malocclusion. The Herbst functional appliance is one appliance commonly used to address Class II malocclusions. Pancherz, et al. assessed the effect of chin position and condylar growth with Herbst appliance therapy (Pancherz, Ruf, and Kohlhas 1998), and "signs of condylar remodeling" and rotation of the mandibular body were reported in their study. Several studies have shown a short-term increase in mandibular length following the use of functional appliances (Pancherz 1979; Yang et al. 2016). Animal studies assessing the effect of fixed Herbst appliance on the condyle-fossa relationship (Voudouris, Woodside, Altuna, Kuftinec, et al. 2003) showed a remodeling process in the condyle and fossa complex. Their study was carried out on nonhuman primates and compared their growth pattern to control and sham cases. In their control patients, they reported "bone resorption along the anterior border of the postglenoid spine and deposition along the posterior border". In Herbst patients, the opposite pattern was observed, ie, apposition along the anterior border of the postglenoid fossa and resorption occurred along the posterior border. Similarly, the condylar growth in Herbst patients was in a posterosuperior direction, which was the opposite of what is normally seen as anterosuperior growth.

It is well known that the articular tissue of the TMJ has a great potential for adaptation and change based on functional requirements and demands (Vitral et al. 2007). Some authors have shown a correlation between the morphology of the TMJ and occlusal factors (Mongini and Schmid 1987; O'Byrn et al. 1995), while others have not shown such a correlation (Matsumoto and Bolognese 1995).

The majority of studies so far, has been performed using 2-D cephalometric images and therefore have many limitations, (Durao et al. 2013) such as magnification error, patient orientation error, association error, projection error, machine alignment error and landmark identification error and use of surrogate landmarks (Baumrind and Frantz 1971; Schulze, Gloede, and Doll 2002). Chadwick, et al. compared image distortion and magnification of 3 different 2-D cephalometric systems and concluded that both error sources are machine-dependent and cannot be predicted (Chadwick et al. 2009). Landmark identification error is deemed as the major source of error, and while great variability has been recorded in landmarking of 2-D images compared to gold standard, 3-D imaging has been shown to be within 1 mm of the gold standard (Adams et al. 2004). Strstemann, et al. also compared landmark identification on 3-D images to gold standard and reported less than 1% relative error (Stratemann et al. 2008).

Al-Saleh, et al. tried to evaluate the body of evidence regarding the 3-D changes in the TMJ following Class II correction in a recently published systematic review (Al-Saleh et al. 2015), yet they failed to "establish a conclusive evidence of the exact nature of tissue response" due to the high level of bias in current studies.

More recently, immediate changes in the condyle after Herbst appliance therapy have been assessed 3-dimensionally (Cheib et al. 2016; Souki et al. 2017). Using 3-D superimposition methods, they showed an increase in bone remodeling of the rami and forward and downward movement of the condyles following Herbst therapy.

It has also been reported that different malocclusions or different methods could exhibit differences in remodeling of the condyle and the fossa (Vitral et al. 2007; Vitral et al. 2004; Rodrigues, Fraga, and Vitral 2009).

Despite many 2-D analyses, there has not been a 3-D analysis available to fully assess the condyle and fossa area and their response to the Herbst appliance. The aim of the following study was to evaluate the condyle/fossa area following HG or Herbst appliance therapy using a 3-D analysis in order to better understand how the shape and position of the condyle and fossa might be affected by treatment.

## Materials and methods

Seventy-two subjects were included in this retrospective study. Based on the standard deviation of 1.85 mm in Pancherz, et al.'s study (Pancherz, Ruf, and Kohlhas 1998), a significance level of 0.05 and a power of 0.80 to detect a 1 mm change in condylar position, a sample size of 20 per group was calculated. The study was approved by the institutional review board of the University of Washington for viewing the CBCTs with the names of the patients embedded in the DICOM file.

The samples for this study were collected from two different clinics in California. The first one was a private orthodontic practice (T.B.) that routinely uses Headgear (HG) for Class II correction. The second was the graduate orthodontic clinic at the University of Pacific, which routinely uses the Herbst appliance (HA). In order to obtain the HG sample, all debonded cases in 2016 from the private practice were reviewed. The first 20 consecutive cases that met all the inclusion criteria were chosen for the study. The control group consisted of Class I cases treated at the same office, matched as closely as possible for age and gender.

In order to obtain the Herbst sample for this study, all the cases treated with the Herbst appliance at UOP who met the inclusion criteria were included in this study. 17 patients met the inclusion criteria. The control group consisted of Class I cases treated at UOP matched as closely as possible for age and gender.

## Inclusion criteria

1) CBCT was obtained at the start of orthodontic treatment (T0) and at the completion of orthodontic treatment (T1)
2) Patients were in the age range of 11-18 at the initiation of treatment
3) No history of TMJ fracture or surgery
4) Class II patients defined as presence of at least half cusp Class II molar relationship bilaterally or full cusp Class II unilaterally. Class I patients defined as Class I malocclusion on both sides
5) CBCTs obtained with teeth in maximum intercuspation with the condyle and fossae clearly imaged
6) Class II cases were successfully treated to Class I canine with normal OJ and OB (OJ $\leq$ 2 mm)

## Image Acquisition

CBCTs were taken for all the subjects using an iCat machine (Imagine Sciences International, Hatfield, PA) with a voxel sixe of 0.3 mm. Each volumetric data set was acquired with a 1 sweep; 20-second scan time with a 16.0 cm (diameter) x 13.0 cm (height) extended height field of view at a resolution of 0.3 voxel. All images were collected at 120 kVp and 4 mA based on manufacturer's specification. Xoran (i-CAT software, version 2.1.22) was used to reconstruct and export the raw data as a 14-bit-depth digital imaging and communications in medicine (DICOM) file. All the images that were acquired after 2012 had a scan time of 8.9 seconds and a resolution of 0.3 voxel. The average time between the CBCTs in the Herbst/Class I group and the HG/Class I group are summarized in Table 1.

## Image analysis

The methodology for assessing the condylar position is described by Hatcher, et al. (Hatcher 2015). Stratovan checkpoint software (Stratovan Corporation, Davis, CA) was used to place 3D landmarks and semilandmarks for analysis of the shape, concentricity and position of the condyle and fossa before and after treatment. The steps can be outlined as follows:

1) Brightness and resolution of each image was adjusted to obtain an image that is easily visualized. The TMJs are oriented in Cartesian system to mimic natural head posture.
2) Landmarking the CBCT images: 3 fixed points were marked on the condyle and fossa to orient a 11 x 11 landmark mesh containing semi-landmarks. In order to accurately assess the condylar position changes relative to the skulls, 6 reference points were selected on the skull (Table 1). The definition of the fixed landmarks is outlined in Table 1.
3) Adjusting semi-landmarks: with the help of the landmarks determined in the previous step, a foundation was formed to determine other landmarks on the condyle and the fossa. For a full tracing of the condyle and fossa, 118 generated points were defined for the condyle and the same number of points were defined for the fossa. The semi-landmarks can only be adjusted along the long axis in the axial/coronal plane. The software then created a condyle and fossa template (Figure 1). All 118 points were reviewed and adjusted to ensure proper landmarking using multiplanar sectional images of the TMJs. The condyle mesh generates 1 to 1 correspondence to the fossa mesh (121 distance measurements). The 3-D coordinates of all landmarks were then exported into a population pool for analysis. A calibrated examiner (DH) reviewed all the tracings to ensure proper landmark selection for all CBCT images.

4) Two separate landmarking sessions were completed as follows: 1) 11 x 11 landmarking of condyle and fossa for each joint independently to determine size, shape and condyle/fossa spatial relationships at T0 and T1. 2) 5 x 5 landmarking of condyle/fossa and spatial relationships of both TMJs simultaneously and 2 midline and 4 bilaterally paired skull base landmarks to quantify the T0-T1 spatial positioning of condyles and fossa (Figure 2). The list and definition of all the landmarks used for 3-D tracing of the CBCTs is provided in Table 1.

The length of the mandible was measured in InVivo software (Anatomage Corporation, San Jose, CA). 2D lateral cephs were exported out of the CBCTs. In order to adjust for patient positioning error, the superior wall of the orbit, cribriform plate and posterior border of the condyles were used as reference lines in 3 planes of space. Opacity and brightness of each image was adjusted until the superior border of the condyle was clearly visible. The distance from Condylion to Pogonion was measured in each case before and after treatment.

## Statistical analysis

*Quantifying condylar shape change*

In order to analyze the changes in condyle shape irrespective of differences in location, size and orientation of each condyle, generalized Procrustes analysis (GPA) was used. This method projected each specimen into a single shape space using an iterative least-squares approach (Gower 1975; Rohlf and Slice 1990). Superimpositions were performed in MorphoJ v. 1.06d (Klingerberg 2011). Since the landmarks were collected in a different order for left and right condyles, it was not possible to superimpose the two sides simultaneously. The analyses, therefore, were carried out for each condyle separately. Statistical results are presented for both sides, but the figures in this article only represent the right side.

The effects of size and age on condylar shape change were tested using ordinary least-squares regression of Procrustes distance on either age or the log of centroid size for both Class I and Class II cases were tested.

Differences between group mean shapes were first assessed using permutation tests designed after the protocols recommended by McNulty et al. (McNulty, Frost, and Strait, 2006). The following groups were tested in this way: Class I and Class II (untreated) groups; Class I and Class II (treated) groups; and, treated Class II Herbst and Class II HG groups. Principal component analysis (PCA) was also used to visualize the distribution of specimens in shape space, and to reduce the number of variables for further analyses.

Because PCA showed a much greater variation between the individuals in each group that among different groups, a stepwise discriminant analysis was performed on the principal components representing 95% of the sample variance to find the best axis distinguishing Class I from Class II untreated individuals (Kimmerle, Ross, and Slice 2008). The identified variables were subsequently used in a discriminant function analysis (DFA) of the same groups (Class I vs. Class II untreated), with treated Class II cases then projected on to the resulting discriminant function (Figure 4). This approach is designed to maximize shape differences between Class I and Class II (untreated) groups, and hence statistical differences between them are more likely to be identified. However, the placement of treated Class II individuals – those not included in the DFA calculations – on the discriminant function represents their condyle shapes relative to the shape differences between Class I and untreated Class II groups.

*Quantifying differences in condyle position*

The second landmarking protocol included using 50 landmarks on the condyle and the fossa as well as 7 relatively stable landmarks on the skull. These landmarks were used to assess the position of the condyle relative to glenoid fossa and cranial base. The mean distance between the landmarks on the superior aspect of the condyle to their corresponding points on the fossa were used to define the superoinferior position of the fossa. The mean distance between five anterior-most landmarks on the condyle base to their corresponding points on the fossa were used to define the anteroposterior position of the condyle. This analysis was carried out for both left and right condyles and fossae.

In order to assess the position of the condyle relative to cranial base, a centroid was defined for each condyle by using the mean of all the landmarks. A line connecting basion and malleus was used to represent the position of the cranial base. All the landmarks were projected on mid-sagittal plane and the distance between the centroid and the basion-malleus line was measured.

Analysis of variance (ANOVA) was used in all cases to detect differences within each group and between different groups. No further analyses were required since no significant differences were identified between different groups

All statistical analyses of fossa shape, size, and position were generated using SAS/STAT and SAS/IML software, version 9.3 of the SAS System for Windows (Copyright © 2002-2010, SAS Institute Inc., Cary, NC, USA).

## Results

The descriptive analysis of all the samples is outlined in Table 2. As expected, the cases were well matched on age and gender. Seven cases were dropped from the HG group due to the poor quality of CBCT either at T0 or T1. One case was dropped from the Herbst group due to the low quality of CBCT at T0. In order to match the Class I cases, the same number of matched patients were dropped from these groups. The mean configuration of the shape of the condyle in all groups is shown in Figure 3.

All the cases in the Herbst group had bilateral full cusp Class II malocclusion, 2 were Division 2, and the rest were Division 1 malocclusion.

In the HG group, 4 cases had bilateral full cusp Class II malocclusion. 10 were bilateral end-on Class II and 3 were Class II subdivision cases.

The effects of size and age on condylar shape change were tested using ordinary least-squares regression of Procrustes distance on either age or the log of centroid size for both Class I and Class II cases were tested.

Evaluating the effect of treatment on the shape of the condyle

To look at possible effects of age and size on the magnitude of shape change resulting from interventions, Procrustes squared distances were computed for each individual between Initial and Final condyle shapes. The resulting distances were regressed against age and the log of centroid size to test for correlations.

- No significant age effect was observed on the amount of shape change between initial and final scans
- No significant size effect was observed on the amount of shape change between initial and final scans for Class II individuals.

The correlation between age and size on the shape of the condyle is summarized in Table 3. The R-squared values indicate minimal correlation, and the only significant finding was for age and shape change on the left side. However, the r-squared value was only 0.33.

Figure 3 shows the overall distribution shape of all samples.

The PCA plot demonstrates almost complete overlap between Class I and Class 2 individuals, indicating similar shape variation in both groups (Figure 4).

Table 4 summarizes the results of the permutation test assessing shape differences between group means. No significant differences were found between any of the groups except for Class I and initial Class II cases on the left side (P=0.032)

Evaluating the position of the condyle relative to the fossa before and after treatment

In order to assess the vertical position of the condyle relative to the fossa, the average of the distances from landmarks on the articular surfaces of the condyles to their respective points on fossa were measured. In order to assess the anterior position of the condyle relative to the fossa, the average of distances from the middle five semilandmarks on the anterior condyle base was measured to their respective points on the fossa. There were no significant changes either in the vertical or anterior position of the condyle relative to the fossa from initial to final in any of the groups. The results are summarized in Table 5.

Evaluating the changes in the position of the condyle relative to cranial base

The position of the condyle was represented as the centroid of 3-D landmarks for the condyle. Condyle centroids along with cranial base landmarks were superimposed together by GPA in morphoJ and the landmarks were projected onto the midsagittal plane to assess anteroposterior position of condyle. The anteroposterior position was judged as the distance of the condyle centroid from a line between the basion and malleus landmarks. There were no significant differences in any of the three groups from initial to final (P= 0.100 in Class I group, P=0.48 in Herbst and P=0.22 in HG group).

We also intended to assess the changes in the shape of the fossa that accompanied Class II correction. However, due to the differences in size, shape and anatomic locations of the condyle relative to fossa, it was not possible to establish congruency between the condyle and fossa in landmarking. Therefore, there were many missing semi-landmarks on the fossa and that made analysis of the shape of the fossa impossible.

The results of the changes in the length of the mandible are reported in Tables 6 and 7. There were no significant differences in the changes in the length of the mandible between Class II and control groups.

## Discussion

In this retrospective study, the effects of Herbst or HG treatment on the shape and position of the condyle relative to the fossa and cranial base were assessed. The aims of this study were fourfold; first to assess the changes in the shape of the condyle, next to assess the changes in the position of the condyle relative to the fossa as well as relative to cranial base, and last to assess the changes in the shape of the fossa. Due to the shape difference between the condyle and fossa, there were some missing landmarks on the fossa, therefore, it was not possible to do a statistical analysis on the changes in the shape of the fossa.

This study incorporates a novel 3-D tracing method to assess the condyle and the fossa. Creation of a 3-D mesh allows for an accurate assessment of the condyle. Most of the previous studies have focused on using 2-D lateral cephalometric images to assess the effects of treatment on the position of the condyle (Baysal and Uysal 2014; Pancherz 1979; Pancherz, Ruf, and Kohlhas 1998; Yang et al. 2016), however, machine alignment error, association error, patient positioning error and landmark identification error all can affect the accuracy of the results. Investigators have recently started using MRI to look at the position of the condyle (Miao et al. 2018), but most of them extract a 2-D lateral cephalograms from the MRI. Two-dimensional analyses do not maximize the information that is gained form 3-dimensional imaging. 3D analysis using CBCT eliminates projection error, association error, patient orientation error, and external orientation error and reduces anatomic identification error. The voxel size of 0.3 mm will create a landmarking error envelope in the range of +/- 0.3 mm. Some investigators have used heat map analysis to assess condylar position in CBCT images (Cheib et al. 2016; Souki et al. 2017). However, statistical analysis cannot be performed on a heat map. Also, heat maps do not control for 6 degrees of freedom between associated anatomies. Therefore, alternative methods are desirable.

Even though 3-D images have been available for several years, we have not been able to fully exploit their 3-D data due to the lack of a proper analytical tool. The current study uses a novel method for 3-D analyses. The Geometric morphometrics technique has just recently been introduced to the field of orthodontics. Huanca, et al. (Huanca Ghislanzoni et al. 2017) used this method, and concluded this new technique can help assess shape variability independent from changes in size. In their study, Huanca et al. reported that using semi-landmarks placed at a pre-determined intervals along the curve of a shape (i.e., condyle or fossa) as the best method of landmarking in geometric morphometrics, which is the exact method used in this study. A total of 242 points were used to map the surface of each condyle and fossa in our study. Geometric morphometric allows for analysis of all the landmarks and proper assessment of the changes in the shape of the condyle. This method uses a collection of landmarks instead of lines and angles, thereby omitting the error that can occur when single landmarks are used.

We tried to evaluate the position of the condyle relative to 7 stable landmarks in the skull. Finding accurate and stable landmarks for the purpose of superimposition has always been a challenge for researchers. Investigators have suggested using point registration on landmarks in the skull that remain mostly unchanged after the age of 7. While it has been stated that none of the skull landmarks are completely accurate, in the absence of a gold standard, they are still acceptable (Jacobson and Sadowsky 2006). We incorporated several relatively stable intracranial landmarks for assessment of the position of the condyle relative to cranial base.

Based on the results of the current study, there were no mean differences between the initial and final positions of the condyles either relative to the cranial base or the fossa. There were also no differences in the final shape of the condyles in Class I and II cases. These results are in contrast with the previously published studies (Cheib et al. 2016; Souki et al. 2017; Voudouris, Woodside, Altuna, Angelopoulos, et al. 2003; Voudouris, Woodside, Altuna, Kuftinec, et al. 2003) which find change in condylar position at the initial and final timepoints. In the present study, all the final CBCTs were obtained upon completion of treatment and removal of all appliances. Therefore, this study contrasts with some previous 3-D studies because these results represent a longer-term assessment of the condyle rather than an immediate, short-term analysis (Souki et al.

2017; Cheib et al. 2016). In the aforementioned studies, the changes in the condyle were assessed immediately after placement or removal of the Herbst appliance. In our study, there was an average of 20 months between the removal of Herbst appliance and the final CBCT image acquisition. Therefore, it could be speculated that early detection of changes that occur in the condyle are temporary and disappear after a period of time. According to Proffit, even though there is an acceleration in mandibular growth during the period of functional appliance treatment, "a long-term increase in size is difficult to demonstrate."(Proffit, Fields, and Sarver 2012) It could be speculated that if functional appliances lead to movement of the condyle out of the fossa, it is a temporary dislocation that will resume its original position after a period of time.

In a long-term 2-D study, Pancherz, et al. compared a group of cases treated with Herbst appliance and compared them to Bolton standards (Pancherz, Ruf, and Kohlhas 1998).They reported that in Herbst cases, the mandible was positioned 0.9 mm more backward compared to the control Bolton group after 3 years, even though some drastic positive changes were seen immediately after treatment. Considering sources of error using 2D cephalometric imaging, it is doubtful that 0.9 mm accuracy can be obtained, especially due to the fact that an arbitrary point in the area of condylar head was used as one of the landmarks.

In Voudouris, et al.'s studies (Voudouris, Woodside, Altuna, Angelopoulos, et al. 2003; Voudouris, Woodside, Altuna, Kuftinec, et al. 2003), the experimental animals were followed for 6, 12 and 18 weeks before being sacrificed for histological evaluation. They showed an increase in remodeling, specifically within the first 6 weeks. They concluded that 18 weeks corresponds to 6 months in humans. When the changes in the length of the mandible were compared between Class II and control groups, no significant differences were reported.

It can be postulated that some remodeling happens at the first stages of Herbst placement, but over time that the condyle is "re-seated" in its original position and the dentoalveolar changes are what maintain a corrected occlusion. Pancherz, et. al, showed a significant amount of improvement in condylar and chin position in Herbst patients during the first 6 months of treatment (Pancherz, Ruf, and Kohlhas 1998). However, this change was reversed between 6 to 36 months post-treatment. In contrast, the control cases showed either an equal or increased amount of growth within the same time period. It could be postulated that the condyle starts to "re-seat" in the fossa 6 months after Herbst removal. Voudouris, et al. (Voudouris, Woodside, Altuna, Angelopoulos, et al. 2003; Voudouris, Woodside, Altuna, Kuftinec, et al. 2003) showed that the greatest amount of change in the experimental primates with Herbst appliance was "a restriction in downward and backward direction of growth in the glenoid fossa" which would be the same response in both HG and HA patients. They explained that any relapse might be due to the muscular activity and perimandibular connective tissue that result in re-seating of the condyle back in the fossa. We were not able to assess the changes in the fossa, but it is very possible that the duration of treatment in humans is not enough to overcome the muscular and connective tissue forces.

When all the identified variables were used to plot the differences between Class I cases and untreated Class II cases (Figure 5), a trend was seen in which all untreated Class II patients would start with a condylar shape different than Class I patients. However, they all showed a similar shape to Class I cases at the end of treatment. We evaluated the changes in their shape to see what areas changed the most. The analysis of the post-treatment tracings showed a shape change in the condyle, where the medial pole of the condyle effectively rotates anteriorly and the lateral pole rotates posteriorly. This shape change might be occurring by regressive remodeling in the anterior surface of the lateral pole of the condyle and progressive remodeling of the posterior surface of the medial pole. The changes in the shape of the condyle and their comparison to Class I cases are demonstrated in Figures 6 and 7. While the shape changes were statistically significant, they were also subtle, and further investigation into potential 3-D shape changes of the condyle during orthodontic treatment are warranted.

There were some limitations to the current study. We used all the patients that met the inclusion criteria from University of Pacific for our Herbst group. However, Herbst treatment was stopped in 2016 and only a limited number of patients (N=17) could be recruited for this study. This had resulted in our study being slightly underpowered.

The long period of time between Herbst removal was also a limitation. Ideally, CBCTs taken before treatment, immediately after HG or Herbst treatment and at completion of all treatment would be most informative regarding any changes of the condyles and fossae.

This was a retrospective study, and that could introduce some bias into the results of the study. A prospective study design is preferred, however, conducting a randomized clinical trial might face some ethical issues.

It would be ideal to have a third group of Class II untreated patients to compare them against the current samples on the linear discriminant function analysis.

## Conclusion

1) There were significant differences in the shape of the condyle between Class II untreated and Class I cases. There is more internal rotation of the mediolateral long axis of the untreated Class II condyle. Relative to the coronal plane, the internal rotation indicates the degree that the lateral pole is anterior to the medial pole of the condyle.
2) There were no differences in the position of the condyle relative to the fossa before and after Class II correction with HG or Herbst appliances, or between Class I and Class II cases.
3) There were no differences in the position of the condyle relative to the cranial base before and after Class II correction with HG or Herbst, or between Class II and Class I cases.
4) If the condyle is postured anteriorly following Herbst treatment, it appears to eventually become "re-seated" in its original position.

**Table 1**. Definition of the condyle, fossa and skull landmarks used for 3-D tracing of the CBCTs

| Landmark | Definition |
|---|---|
| **Lateral pole of the condyle** | The lateral height of contour of the widest mediolateral part of the condyle in the coronal view |
| **Medial pole of the condyle** | The medial height of contour of the widest mediolateral part of the condyle in the coronal view |
| **Distal aspect of the condyle** | The distal height of contour of the condyle midway between medial/lateral poles where the cortication tapers off to even thickness in the sagittal view |
| **Malleus** | Following skull orientation (SO) the superior-most point on the malleus of the middle ear |
| **Post. Nasal Spine (PNS)** | Most posterior midline extension of hard palate |
| **Foramen Spinosum (FS)** | Medial-most and inferior-most between FS |
| **Vaginal Process** | Inferior most point in the vaginal process |
| **Medial Fossa Fissure** | |
| **Zygomaticotemporal Suture** | The lateral and inferior most point of the zygomaticotemporal suture |
| **Basion** | Most posterior midline extension of the clivus |

**Table 2**. Descriptive analysis of the subjects of the study

| Group | Age | Sex | Duration | Elastics use | Ext/Non ext |
|---|---|---|---|---|---|
| **Cl I PP** | Range=14-18 YO<br>Avg=16.4<br>SD=1.04 | F=11<br>M=6 | Range=2.3-4<br>Avg=3.1<br>SD=1.5 | Yes=14<br>No=3 | Non-ext=13<br>Ext=4 |
| **HG PP** | Range=13.3-17.5<br>Avg=15.9<br>SD=1.3 | F=11<br>M=6 | Range=2.1-3.9<br>Avg=2.8<br>SD=1.3 | Yes=14<br>No=3 | Non ext=13<br>Ext=4 |
| **Cl I UOP** | Range=9-16<br>Avg=14<br>SD=1.1 | F=10<br>M=6 | Range=1.7-4.2<br>Avg=3.05<br>SD=1.1 | Yes=11<br>No=6 | Non ext=16<br>Ext=0 |
| **HA UOP** | Range=13.1-14.9<br>Avg=12.8<br>SD=1.2 | F=10<br>M=6 | Range=1.2-2.6<br>Avg=3.05<br>SD=1.2 | Yes=11<br>No=6 | Non ext=16<br>Ext=0 |

PP: Private practice, HG: Headgear, HA: Herbst appliance, Avg: Average, SD: Standard deviation

**Table 3**. Relationship between age and size on the shape changes of the condyle

| | Age | | | Size | | |
|---|---|---|---|---|---|---|
| | | $R^2$ | p | | $R^2$ | p |
| **RIGHT** | Class I | 0.0395 | 0.2314 | Class I | 0.0166 | 0.4405 |
| | Class II | 0.0433 | 0.2302 | Class II | 0.0919 | 0.0917 |
| **LEFT** | Class I | 0.3343 | 0.0003 | Class I | 0.0265 | 0.3500 |
| | Class II | 0.0220 | 0.4118 | Class II | 0.0017 | 0.8304 |

**Table4.** Results of permutation tests assessing shape differences between group means.
Right side

| | | Procrustes distance | P |
|---|---|---|---|
| **Class I** | Class II (untreated) | 0.0263 | 0.9160 |
| | | | |
| **Class I** | Class II (treated) | 0.0238 | 0.9760 |
| | | | |
| **Class II HA (treated)** | Class II HG (treated) | 0.0442 | 0.8202 |

Left side

| | | Procrustes distance | P |
|---|---|---|---|
| **Class I** | Class II (untreated) | 0.0504 | 0. 0320 |
| | | | |
| **Class I** | Class II (treated) | 0.0390 | 0.3037 |
| | | | |
| **Class II HA (treated)** | Class II HG (treated) | 0.0753 | 0.1029 |

HA: Herbst appliance, HG: Headgear

**Table 5**. Changes in the vertical and anteroposterior position of the condyle relative to the fossa

| | Vertical space | | Horizontal space | |
|---|---|---|---|---|
| | F | P | F | P |
| **Class I** | 2.09 | 0.156 | 3.67 | 0.0637 |
| **Class II HA** | 0.14 | 0.715 | 0.01 | 0.922 |
| **Class II HG** | 0.07 | 0.797 | 1.55 | 0.226 |

HA: Herbst appliance, HG: Headgear

**Table 6.** Mean, standard deviation, standard error, and the mean difference in the length of the mandible between different groups

| | Mean (mm) | Standard deviation | Standard error | Mean difference(mm) |
|---|---|---|---|---|

| | | | | |
|---|---|---|---|---|
| **HA UOP initial** | 101.5 | 5.91 | 1.43 | 4.5 |
| **HA UOP Final** | 106.0 | 5.91 | 1.43 | |
| **Class I UOP initial** | 107.4 | 6.3 | 1.52 | 4.1 |
| **Class I UOP final** | 111.5 | 6.6 | 1.6 | |
| **HG PP initial** | 97.7 | 5.7 | 1.4 | 8.4 |
| **HG PP final** | 106.3 | 7.4 | 1.8 | |
| **Class I PP initial** | 102.1 | 5.8 | 1.4 | 7.5 |
| **Class I PP final** | 109.7 | 5.1 | 1.2 | |

PP: Private practice, HG: Headgear, HA: Herbst appliance, Avg: Average, SD: Standard deviation

**Figure 1**. Creating a condyle-fossa template following 3-D tracing

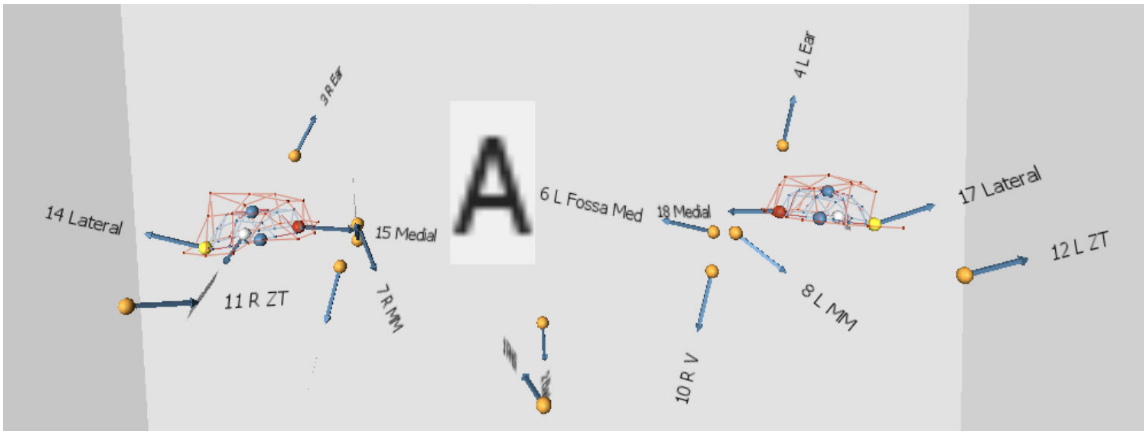


**Figure 2**. 5x5 landmarking of the fossa and condyle, skull landmarks are added. The condyle-fossa mesh and landmarks are exported

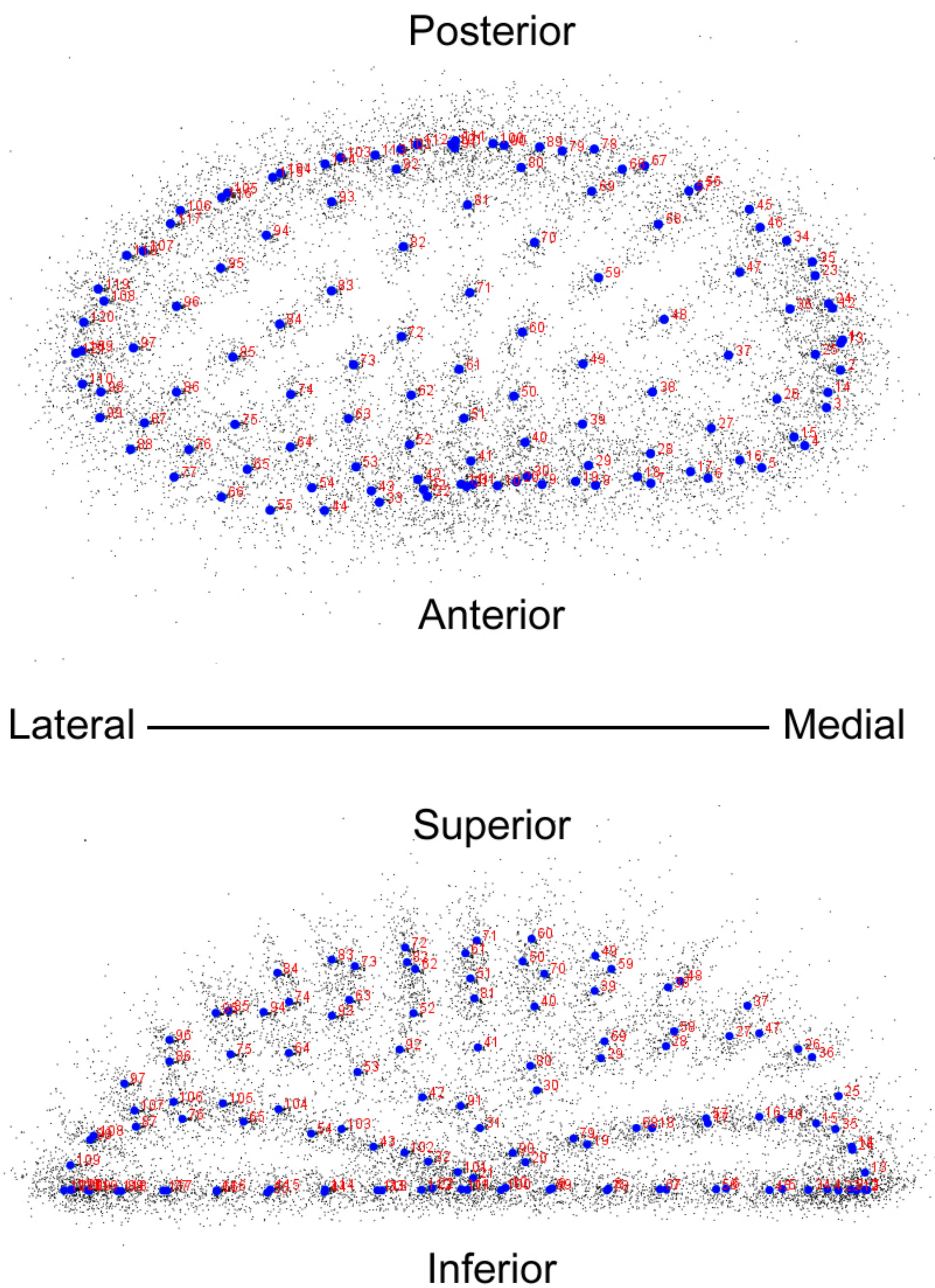


**Figure 3**. The mean configuration of the shape of the condyle rendered after landmarkin

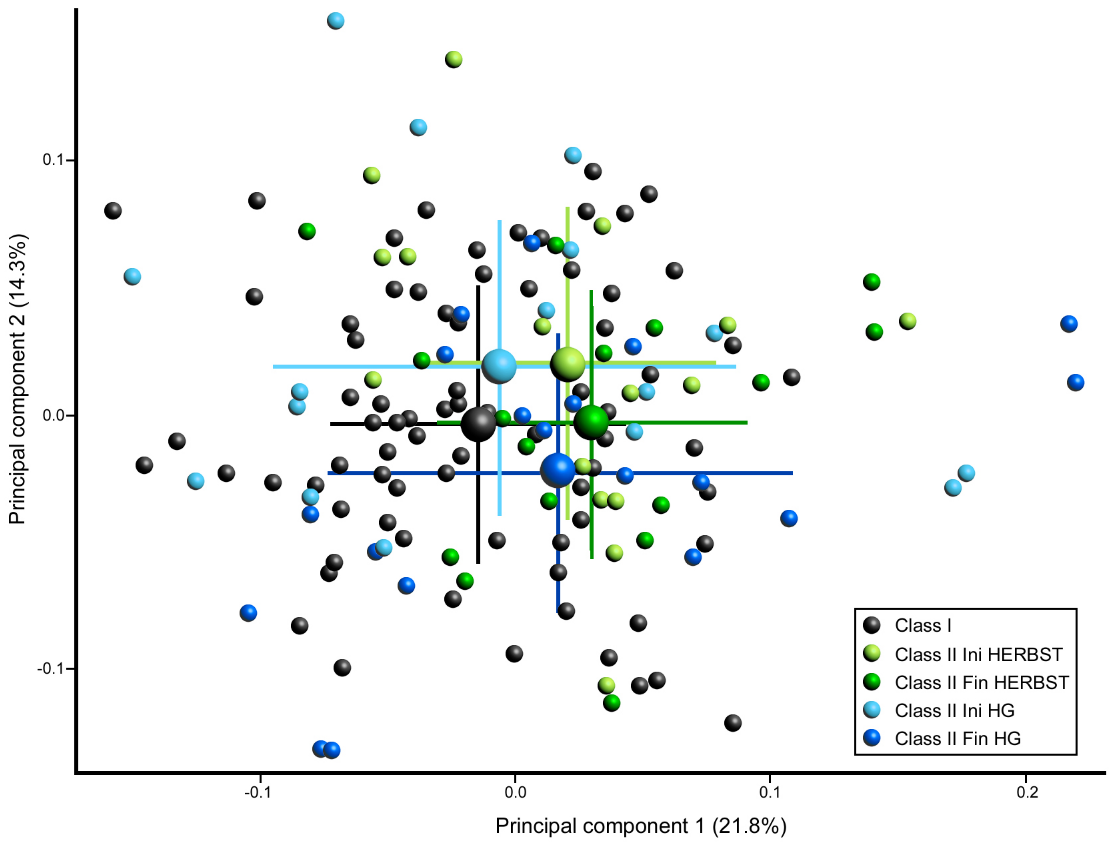


**Figure 4**: Bivariate plot of first two principal components computed form the covariance matrix of aligned coordinates from the right condyle. Lines connecting observations join Class II individuals before and after treatment. On the x-axis PC1, on the y-axis PC2 from Principal component analysis.

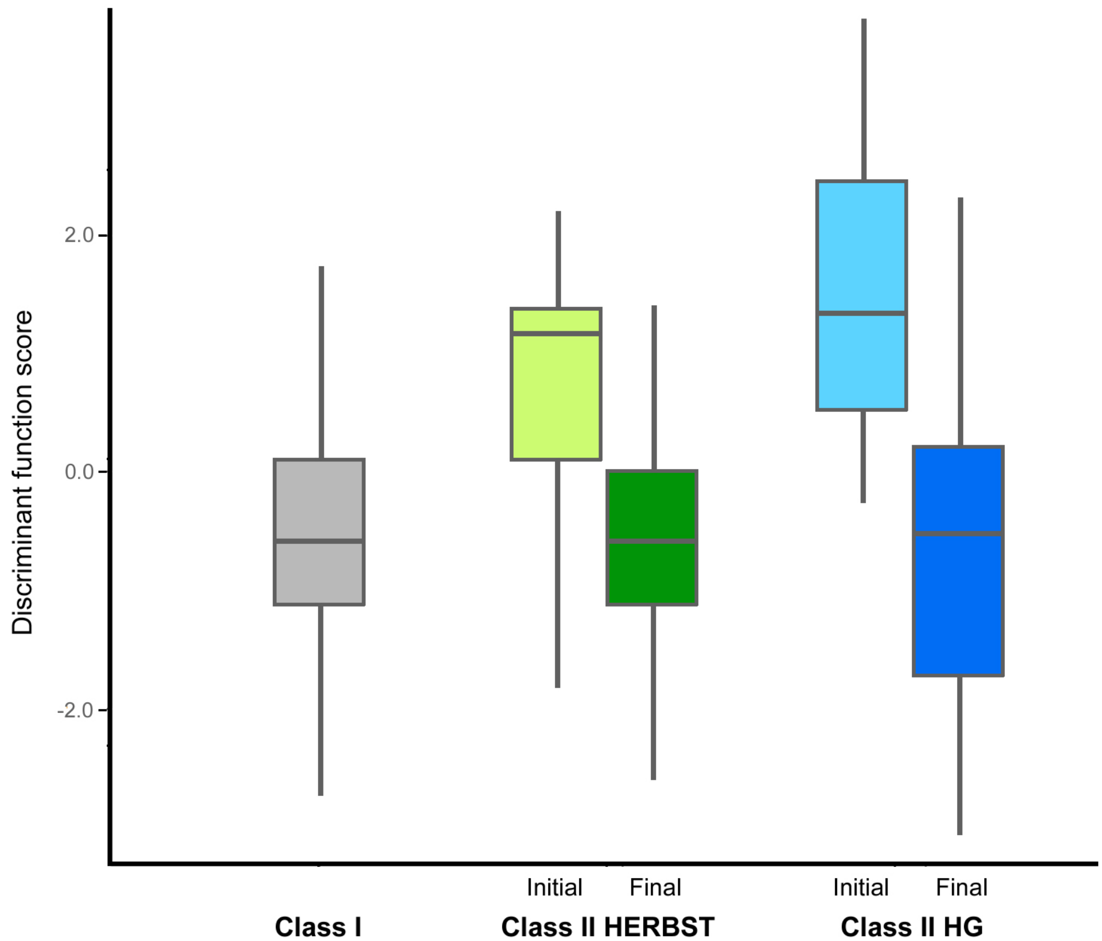


**Figure 5**. Box-and-whisker plot of discriminant function scores for Class I vs. Class II individuals. Treated Class II individuals (final) were not included in discriminant function calculations, but instead plotted onto the resulting discriminant function. Right side condyle is shown.

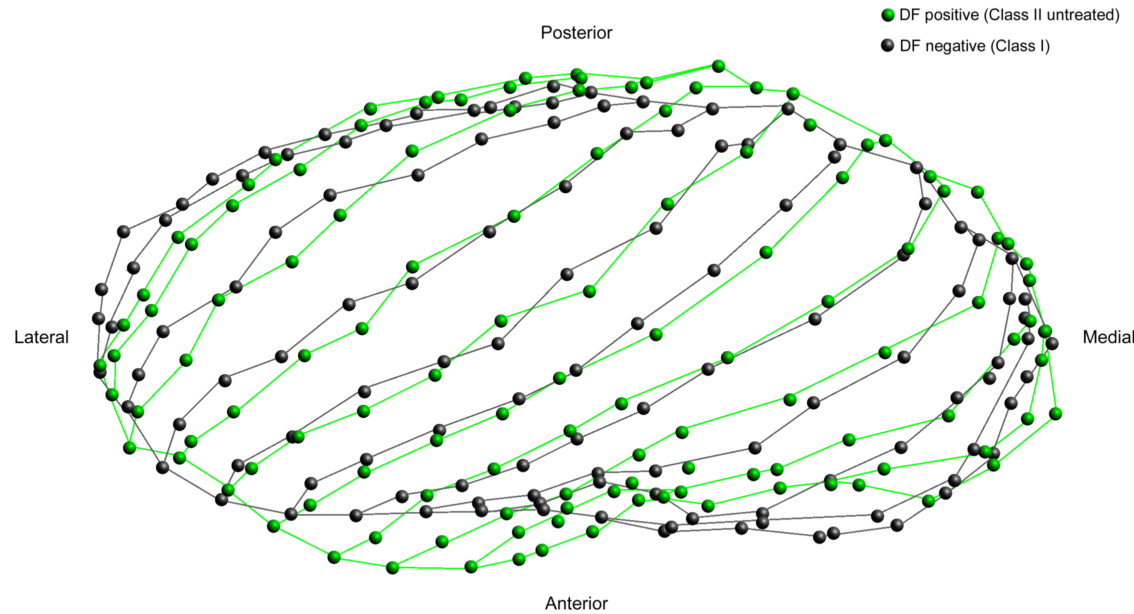


**Figure 6**. The overall difference in the shape of the condyle between Class II untreated and Class I cases (superior view of the condyle).

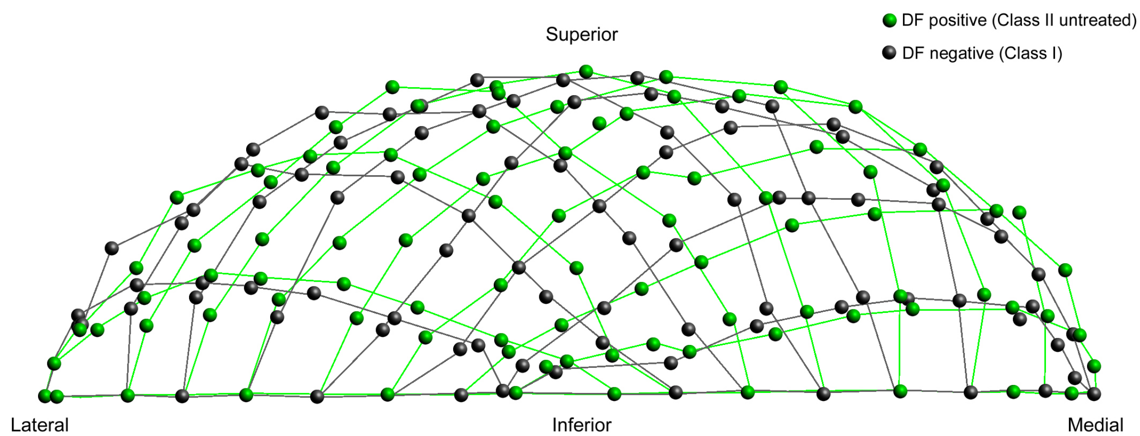


**Figure 7**. Figure 6. The overall difference in the shape of the condyle between Class II untreated and Class I cases (sagittal view of the condyle).

## References


Adams, G. L., S. A. Gansky, A. J. Miller, W. E. Harrell, Jr., and D. C. Hatcher. 2004. 'Comparison between traditional 2-dimensional cephalometry and a 3-dimensional approach on human dry skulls', *Am J Orthod Dentofacial Orthop*, 126: 397-409.

Al-Saleh, M. A., N. Alsufyani, C. Flores-Mir, B. Nebbe, and P. W. Major. 2015. 'Changes in temporomandibular joint morphology in Class II patients treated with fixed mandibular repositioning and evaluated through 3D imaging: a systematic review', *Orthod Craniofac Res*, 18: 185-201.

Baumrind, S., and R. C. Frantz. 1971. 'The reliability of head film measurements. 2. Conventional angular and linear measures', *Am J Orthod*, 60: 505-17.

Baysal, A., and T. Uysal. 2014. 'Dentoskeletal effects of Twin Block and Herbst appliances in patients with Class II division 1 mandibular retrognathy', *Eur J Orthod*, 36: 164-72.

Chadwick, J. W., R. N. Prentice, P. W. Major, and E. W. Lam. 2009. 'Image distortion and magnification of 3 digital CCD cephalometric systems', *Oral Surg Oral Med Oral Pathol Oral Radiol Endod*, 107: 105-12.

Cheib, P. L., A. Cevidanes, A. Ruellas, L. Franchi, W. Braga, D. D. Oliveira, and B. Souki. 2016. 'Displacement of the mandibular condyles immediately after Herbst Appliance Insertion - 3D assessment', *Turkish Journal of Orthodontics*, 29: 31-7.

Durao, A. R., P. Pittayapat, M. I. Rockenbach, R. Olszewski, S. Ng, A. P. Ferreira, and R. Jacobs. 2013. 'Validity of 2D lateral cephalometry in orthodontics: a systematic review', *Prog Orthod*, 14: 31.

Gower, J.C. 1975. 'Generalized Procrustes analysis', *Psychometrika*, 40: 33-51.

Hatcher, D. 2015. 'A novel three-dimensional analysis to evaluate the temporomandibular joint space and shape', *American Journal of Orthodontics and Dentofacial Orthopedics*, In press.

Huanca Ghislanzoni, L., R. Lione, P. Cozza, and L. Franchi. 2017. 'Measuring 3D shape in orthodontics through geometric morphometrics', *Prog Orthod*, 18: 38.

Jacobson, A., and P.L. Sadowsky. 2006. 'Superimposition of cephalometric radiograph.' in A. Jacobson and R.L. Jacobson (eds.), *Radiographic cephalometry from basic to 3-D imaging* (Quintessence publishing Co.: Hanover park, IL).

Kimmerle, E.H., A. Ross, and D. Slice. 2008. 'Sexula dimorphism in America: Geometrics Morphometric analysis of the craniofacial region', *J Forensic Science*, 5: 54-57.

Klingerberg, C.P. 2011. 'MorphoJ; an integrated software package for geometric morphometrics', *Molecular Ecology Resources*, 11: 353-57.

Matsumoto, M. A., and A. M. Bolognese. 1995. 'Bone morphology of the temporomandibular joint and its relation to dental occlusion', *Braz Dent J*, 6: 115-22.

McNulty, K.P., S.R. Frost, and D.S. Strait. 2006. 'Examining affinities of the Taung child by developmental simulations', *Journal of Human evolution*, 51: 247-96.

Miao, M. Z., B. Wang, D. Wu, S. Zhang, S. Wong, O. Shi, A. Hu, L. Mao, and B. Fang. 2018. 'Temporomandibular joint positional change accompanies post-surgical mandibular relapse-A long-term retrospective study among patients who underwent mandibular advancement', *Orthod Craniofac Res*, 21: 33-40.

Mongini, F., and W. Schmid. 1987. 'Treatment of mandibular asymmetries during growth. A longitudinal study', *Eur J Orthod*, 9: 51-67.

Nanda, Ravindra. 2005. *Biomechanics and esthetics strategies in clinical orthodontics* (Elsevier: St. Louis, Missouri).

O'Byrn, B. L., C. Sadowsky, B. Schneider, and E. A. BeGole. 1995. 'An evaluation of mandibular asymmetry in adults with unilateral posterior crossbite', *Am J Orthod Dentofacial Orthop*, 107: 394-400.

Pancherz, H. 1979. 'Treatment of Class II malocclusions by jumping the bite with the Herbst appliance. A cephalometric investigation', *American Journal of Orthodontics*, 76: 423-42.

Pancherz, H., S. Ruf, and P. Kohlhas. 1998. '"Effective condylar growth" and chin position changes in Herbst treatment: a cephalometric roentgenographic long-term study', *Am J Orthod Dentofacial Orthop*, 114: 437-46.

Proffit, W. R., H.W. Fields, and D.M. Sarver. 2012. *Contemporary orthodontics* (Mosby).

Rodrigues, A. F., M. R. Fraga, and R. W. Vitral. 2009. 'Computed tomography evaluation of the temporomandibular joint in Class II Division 1 and Class III malocclusion patients: condylar symmetry and condyle-fossa relationship', *Am J Orthod Dentofacial Orthop*, 136: 199-206.

Rohlf, F.J., and D. Slice. 1990. 'Extension of the Procrustes method for the optimal superimposition of landmarks', *syst Biol*, 39: 40-59.

Schulze, R. K., M. B. Gloede, and G. M. Doll. 2002. 'Landmark identification on direct digital versus film-based cephalometric radiographs: a human skull study', *Am J Orthod Dentofacial Orthop*, 122: 635-42.

Slice, D.E. 2001. 'Landmark coordinates aligned by Procrustes analysis do not lie in Kendall's shape space', *Systematic Zoology*, 50: 141-49.

Slice, D.E., F.L. Bookstein, L.F. Marcus, and F.J. Rohlf. 1996. *Appendix I- A glossary for geometric morphometrics* (Plenum: New York).

Souki, B. Q., P. L. C. Vilefort, D. D. Oliveira, I. Andrade, Jr., A. C. Ruellas, M. S. Yatabe, T. Nguyen, L. Franchi, J. A. McNamara, Jr., and L. H. S. Cevidanes. 2017. 'Three-dimensional skeletal mandibular changes associated with Herbst appliance treatment', *Orthod Craniofac Res*, 20: 111-18.

Stratemann, S. A., J. C. Huang, K. Maki, A. J. Miller, and D. C. Hatcher. 2008. 'Comparison of cone beam computed tomography imaging with physical measures', *Dentomaxillofac Radiol*, 37: 80-93.

Vitral, R. W., M. R. Fraga, R. S. de Oliveira, and J. C. de Andrade Vitral. 2007. 'Temporomandibular joint alterations after correction of a unilateral posterior crossbite in a mixed-dentition patient: a computed tomography study', *Am J Orthod Dentofacial Orthop*, 132: 395-9.

Vitral, R. W., S. Telles Cde, M. R. Fraga, R. S. de Oliveira, and O. M. Tanaka. 2004. 'Computed tomography evaluation of temporomandibular joint alterations in patients with Class II division 1 subdivision malocclusions: condyle-fossa relationship', *Am J Orthod Dentofacial Orthop*, 126: 48-52.
Voudouris, J. C., D. G. Woodside, G. Altuna, G. Angelopoulos, P. J. Bourque, C. Y. Lacouture, and M. M. Kuftinec. 2003. 'Condyle-fossa modifications and muscle interactions during Herbst treatment, Part 2. Results and conclusions', *Am J Orthod Dentofacial Orthop*, 124: 13-29.
Voudouris, J. C., D. G. Woodside, G. Altuna, M. M. Kuftinec, G. Angelopoulos, and P. J. Bourque. 2003. 'Condyle-fossa modifications and muscle interactions during herbst treatment, part 1. New technological methods', *Am J Orthod Dentofacial Orthop*, 123: 604-13.
Yang, X., Y. Zhu, H. Long, Y. Zhou, F. Jian, N. Ye, M. Gao, and W. Lai. 2016. 'The effectiveness of the Herbst appliance for patients with Class II malocclusion: a meta-analysis', *Eur J Orthod*, 38: 324-33.